Optical Spectra of Unfolded Proteins: A Partially Ordered Polymer Problem

Timothy A. Keiderling, Qi Xu*

Department of Chemistry, University of Illinois at Chicago, 845 W. Taylor St. (m/c 111), Chicago, IL 60607-7061, USA
E-mail: tak@uic.edu

Summary: Proteins are hetero-sequence polypeptides with complex folded structures whose topology and structural details are vital to their biological function. In this paper, uses of electronic circular dichroism (ECD) in the uv, infrared (IR) absorption and its chiroptical variant, vibrational circular dichroism (VCD) for study of residual structure in peptide models and unfolded proteins under various conditions are addressed. The complementary information gained from analysis of the short range vibrational coupling (with IR and VCD) vs. long range dipole coupling (from ECD) allow detection of partial ordering. The vibrational techniques show an ability to detect local order often missed by ECD (or fluorescence). Perturbation with thermal and solvent variation can then probe stabilities. Furthermore the rapid timescales allow such spectra to follow dynamic changes. Examples from protein folding of cytochrome c and various beta containing proteins are given.

Keywords: circular dichroism; fluorescence; infrared spectroscopy; proteins; stopped-flow

Introduction

Unfolded proteins and unstructured peptides form thermodynamic states critical to the overall protein-folding problem by representing possible initial states in the folding process (or final states in unfolding). However, they are intrinsically poorly defined and evidence is building from various techniques[1] that many of these "unfolded states" have significant local order. Thus studies of how the fold develops, what partially ordered intermediates lie on the path and what are the energetics and dynamics of attaining that fold for both peptides and proteins have become a vibrant area of research in biophysics.

Most physical techniques commonly used for protein conformational studies have a structurally sensitive response. If different residues are in a variety of local conformations, but these are the same in each molecule, such as in the native state, spectra can define conformation, dependent on resolution. However, for the unfolded state any given residue may be in several different local

 DOI: 10.1002/masy.200550202

states. This ensemble and dynamic disorder could pose a problem for site-specific order-sensitive techniques such as x-ray and NMR. On the other hand, optical techniques, although of much less resolution, can provide averaged structure information, which represents all components in the ensemble of structures.

We here address studies of partially ordered proteins with optical spectroscopy, focussing on vibrational infrared (IR) absorption spectroscopy and two chiroptical techniques, electronic and vibrational circular dichroism (ECD and VCD in the uv and IR, respectively). Raman spectroscopy and Raman optical activity (ROA) are also of use in this respect, being even more local order dominated than IR and VCD, but we leave that to other authors.[2-6] Even vibrational spectroscopy is low in resolution, so that site specific information cannot be obtained without isotopic labeling.[7-12] Electronic spectral techniques (including fluorescence) reflect coupling over long range, via electric transition dipoles, while the vibrations interact over shorter ranges, via mechanical coupling. The chirally dependent techniques sense conformation via an interference term making their intensity and sign extremely sensitive to conformational change. Additionally, the vibrational techniques (IR and Raman) have structurally sensitive frequency shifts. Furthermore, optical techniques are very fast, sampling conformations on the pico-second time scale, representing the equilibrium ensemble and directly following fast kinetic changes in the structures, as in folding.

ECD, $\Delta A = A_L - A_R$, of far-uv n-π^* and π-π^* transitions of the amide linkage is a dominant optical technique for protein folding applications.[13-18] Being a differential technique, CD has a bandshape and sign that is sensitive to different secondary structures. Interpretations in terms of secondary structure prediction often use a statistical fit to a reference set of protein spectra,[14,16,18] which for unfolded and partially ordered proteins can be problemetic.[19,20] Fluorescence [21] is the other dominant technique for monitoring folding. It requires chromophores (typically tryptophan in proteins or added emitting ligands), and only yields information about maintence of a stable protein tertiary structure through interactions.

IR and Raman analyses of secondary structure mostly focus on comparative frequency measurement of amide centered modes, which couple through the bonds (mechanically) and are characteristic of different secondary structure types.[3,22-28] Since a polymeric structure does not yield a single frequency for a given structure, but has a large number of coupled modes, one for each local oscillator, a distributed bandshape is observed.[29,30] Most IR studies have focused on

the amide I band, the C=O stretch (amide I, ~1650 cm^{-1}), and sometimes the amide II, while Raman primarily used the amide III (both II and III are NH deformation plus C-N stretch) with some reliance on the amide I.

In principle, using the frequency assigned component approach frees the analyses from constraints due to referencing only globular proteins. However, assigning the frequencies to specific, unique secondary structural types is a severe assumption, since any given conformation will shift in frequency response under the influence of different solvents and residues.[7,31-33] The problem of determining a characteristic spectrum for the unfolded state has been the subject of some studies.[25,29,34-36] Non-uniformity and end effects, which particularly affect partially ordered systems will disperse that contribution over the spectrum.[37-41] To avoid this assignment problem, bandshape-based analyses have also been applied to FTIR and Raman spectra.[37,42-46]

IR resolution and structural sensitivity can be enhanced by use of polarization sensitivity, the simplest of which is linear dichroism (LD) of oriented samples,[47] which can yield bond orientation information for oriented samples. Such methods work for extended polymers, fibrous proteins or membrane bound systems,[48] where macroscopic order is a relevant question, but are not expected to have much application for partially ordered, unfolded states.

VCD couples the frequency resolution of FTIR with the chiroptical stereochemical sensitivity of ECD and adds polarization sensitivity to IR studies of unordered (solution) systems.[49-51] Its counterpart, Raman optical activity (ROA), was developed simultaneously and has been applied to local order problems in proteins [2]. VCD measures the chiral interaction of stretches and bends via the polymer backbone yielding conformationally sensitive bandshapes, but have reduced S/N (ΔA is ~ 10^{-4} - 10^{-5} of the absorbance, A). Interpretation of peptide VCD is enhanced by computational simulation,[7,9,40,52-55] but protein applications use empirically based analyses.[46,50,56,57] While qualitative estimations of protein structure remain of interest for determining the dominant fold type, quantitative estimations of secondary structure content based on empirical band shape analyses are often of more interest.[46,57]

In summary, the combination of these electronic and vibrational spectral techniques can compensate for each other, providing a balance between accuracy and reliability. Partially ordered proteins provide a major challenge for all of these techniques. The short range dependence of VCD and IR (or Raman) is an advantage for identifying residual structure in long-range disordered systems. However the VCD dependence on coupling of neighboring residues

does demand that some structural uniformity over local sequences should remain. By contrast, ECD has residual signals arising from the chirality of the residue C^{α} sites. Hence ECD can develop a strong response consistent with a structure of low order, and VCD and IR can pick out the remains of the previous ordered conformation. It becomes obvious that, despite the fundamental physical differences leading to various advantages for any one technique over another in a given set of circumstances, progress in understanding of complex structures, particularly those with little extended coherence, will come from synthesizing all the data gathered from various techniques.

Experimental Section

Materials. Cytochrome c (horse heart, C-7752) β-lactoglobulin, concanavalin A and carbonic anhydrase were purchased from Sigma and used without further purification. Analytical grade NaCl, sodium phosphate salts and spectroscopic grade methanol were purchased from Fisher Scientific Inc. D_2O, DCl and methanol (d4) were purchased from Cambridge Isotope Laboratories, Inc. and NaOD was prepared by reacting solid Na with D_2O. Trifluoroethanol (TFE) is purchased from Sigma. Deuterated TFE was obtained by distilling TFE 1:5 with D_2O at 77-78°C. Solutions were prepared at 10~30 mg/ml for FTIR and VCD measurement and 0.2-0.3 mg/ml for ECD measurement. All the pH values in this paper represent apparent pH meter readings; no correction was made for solutions prepared in D_2O.

FTIR. Proteins were dissolved directly into D_2O (10–30 mg/ml) or mixed solvents; pH was adjusted with DCl and/or NaOD; and samples were kept overnight to equilibrate deuterium exchange. Solutions were transferred to a demountable cell composed of two CaF_2 windows separated by a 50 μ spacer sealed in a brass ring. The IR absorption spectra were recorded at 4 cm^{-1} nominal resolution as an average of 512 scans using a Digilab FTS-60A (FTIR) spectrometer with a DTGS detector. For the temperature variation studies, these cells were placed in a home-made variable-temperature mount[58] which was temperature controlled using a Neslab RTE-110 water bath, regulated with a thermocouple placed in the outer jacket.

VCD. Amide I' VCD of the same samples were measured on a dispersive instrument which has been described in detail elsewhere.[59,60] VCD were collected on the same samples as for FTIR with ~10 cm^{-1} resolution and a 10 second time constant as the average of 4-6 scans. Baselines

were corrected by substracting identically collected solvent spectra.

CD instrument. Equilibrium and time-resolved CD and fluorescence experiments were performed on a Jasco-810 spectropolarimeter equipped with a Bio-logic stopped-flow accessory. Equilibrium ECD spectra were recorded using 1mm pathlength quartz cell and samples of 0.2-0.3 mg/ml in H_2O adjusted in pH or solvent to obtain various partially folded states. A Neslab RTE-111 water bath was used to control a Jasco variable temperature cell holder. A bandwidth of 1 nm and a response of 2 s were used, to obtain final spectra as an average of 4-8 scans.

Stopped-flow. The stopped-flow module and 2 mm quartz observation cell were thermostatted by means of temperature-controlled water bath. The CD signal was recorded (222 nm) and the total fluorescence signal (>320 nm) was collected at 90° to the 150W Xe-Hg excitation by using a cut-off filter. The normal protocol for the cyt c experiments was mixing 50 µl of 85 µM acid denatured protein solution with 200 µl phosphate buffer containing 0.5 M NaCl at pH=6.8 to give a final solution of 17 µM cyt c and 0.4 M NaCl at pH=6.8, with appropriate variations to achieve alternate initial and final states. Time dependent behaviors were analyzed by fitting the stopped-flow traces with exponential functions using the Bio-Kin32 software (Bio-Logic).

The stopped-flow IR experiments were carried out in a home-made cell with a integral "T" shape mixer. This was placed into the external sample compartment of the Digilab FTS-60A (FTIR) spectrometer with an MCT detector. 10mg/ml of concanavalin A in 10 mM acetic buffer at pH=4.1 was mixed with TFE-OD in the CaF_2 cell with a 100 µm teflon spacer. Spectra were collected with a resolution of 4 cm^{-1} every 80 ms for the fast change and every 5 sec for the slow change. Factor analysis was used to obtain the kinetic changes from the spectra.

Results and discussion

Cytochrome c pH and salt effects. To demonstrate detection of partially ordered states in a protein whose native state is highly helical, we studied the thermal behavior of cytochrome c starting in both the acid denatured and salt-induced molten globule (MG) states.[61-65] The temperature variations (5-80°C) of the IR absorption in the amide I' region of cyt c initially in the MG (pH ~2, 0.5 M NaCl) (a) and the acid denatured (pH ~2) states (b) are shown in Figure 1. The amide I' of cyt c in the molten globule (a) state has a low temperature maximum at 1650 cm^{-1}, which is consistent with a significant α-helix component to the secondary structure and in

agreement with the similarly obtained ECD result in Figure 2.[24] With change of temperature, the IR has a sharp transition at ~50°C, paralleling the decrease of the ECD minimum at 222 nm (loss of helix). A shoulder peak at 1614 cm^{-1} appeared at T=50°C for MG cyt c consistent with the development of cross stranded β-sheets, probably from aggregation.[66,67]

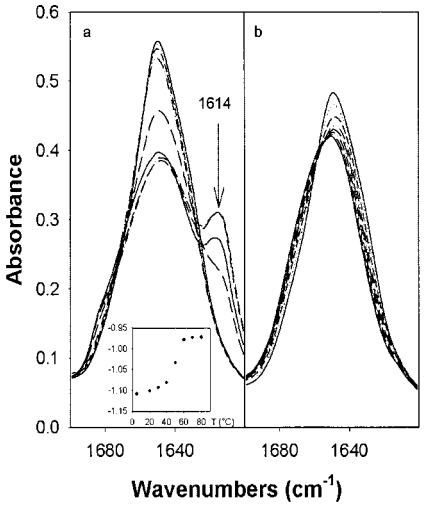

Figure 1. Thermal denaturation FTIR spectra of of ~30 mg/ml Cyt c under (a) molten globule (0.5M NaCl, pH=2) and (b) acid denatured (pH 2) state conditions. In (a), an aggregation induced peak at 1614 cm^{-1} appears at 50°C and its intensity falls back at 80°C, due to precipitation. The intensity change expressed as coefficient loading vs. temperature is plotted as inset.

The acid denatured state behaved quite differently from the MG states in that its amide I' FTIR (Figure 1b) continually changes in shape and frequency and its ECD (Figure 2b) only decreased in magnitude with increase in temperature, both lacking a clear transition. The second derivative of these IR spectra at low temperature had components at 1650 cm^{-1} and 1631 cm^{-1}, which could indicate α-helical and possibly coil or turn contributions, respectively. Confirming this, the VCD spectra, Figure 3b, has the characteristic "W" shape at low temperature, indicating of partial helical structure in the acid denatured state.[50,57] But with increase of temperature, the α-helical band components disappeared quickly, so that by T=40°C only random coil spectral character (1645 cm^{-1}) was left. The thermal denaturation of acid denatured cyt c is reversible when cooled while the MG (and also the native) state become irreversibly aggregated.[68] While the acid denatured cyt c (Figure 3b) at 5°C still has partial ordering in terms of some α-helical content, it is sharply reduced as seen from the decreased intensity of ~1660 cm^{-1} positive VCD peak. With increase of temperature, the two negative VCD peaks merge and become characteristic of a random coil structure by T=40°C.[7,69,70]

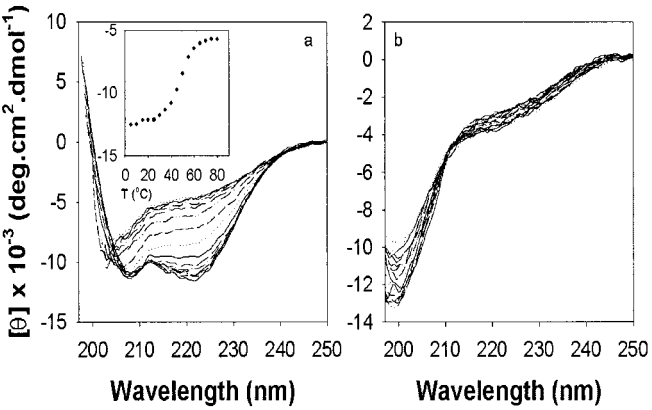

Figure 2. Thermal denaturation ECD spectra of Cyt c under (a) molten globule state and (b) acid denatured state conditions. In (a), the plot inset is ellipticity change at 222 nm.

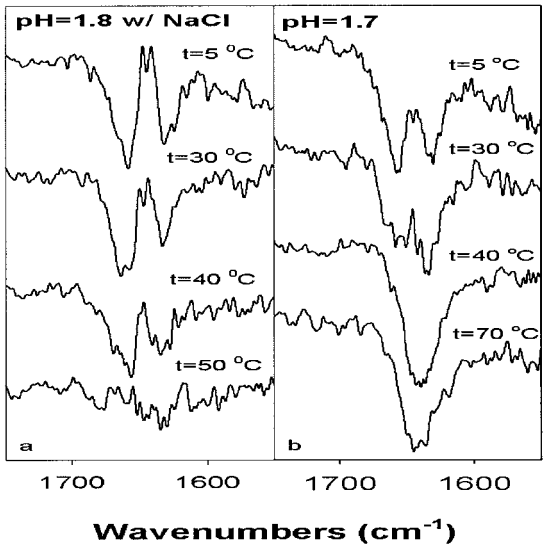

Figure 3. Thermal denaturation VCD spectra of ~30 mg/ml cyt c under (a) molten globule and (b) acid denatured state conditions.

These results demonstrate that various partially ordered states for cyt c are accessible by subjecting the helical bundle native state to solvent (change) perturbation. The acid-denatured state retains partial helical character as seen by use of the short-range sensitivity of VCD,

dependent on through-bond mechanical coupling, a characteristic largely missed by the long range dipole-coupling dominated ECD. By adding salt to this acid-denatured form (added of several anions can shield[71] the protonated residues) the polymer regains partial helical character (Figure 2a). Hence this form is not a native fold but rather a partially ordered sequence lacking

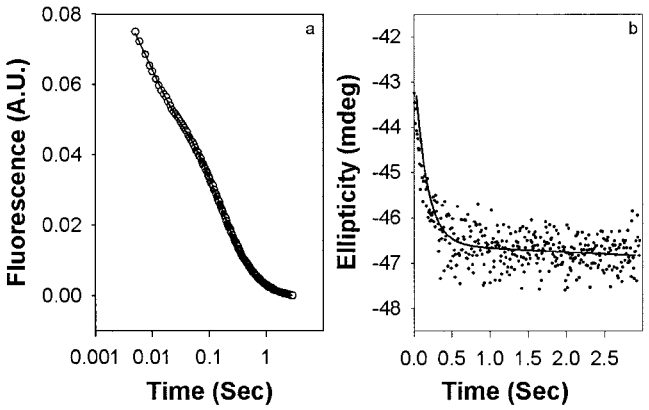

Figure 4. Stopped-flow fluorescence (a) and far-UV CD (b) for refolding of acid denatured cyt c by neutralizing with 100 mM phosphate buffer solution pH=6.8, t=15°C.

tertiary structure.[63-65,72]

The most discriminating spectral test of this partially ordered structure is its thermal stability. In the insets to Figure 1 and 2 are shown thermal profiles of the IR and ECD intensity, showing characteristic sigmoidal loss of the helical character of the MG state in both IR and ECD. By contrast the changes for the acid denatured state (not shown) show no evidence of cooperativity, being monotonic decreases in intensity. It is the combination of techniques, here ECD, VCD and IR, that sorts out these differences and distinguishes these states. Dynamic studies can offer a different look at partially ordered states.

Stopped-flow kinetic experiments. Stopped-flow refolding experiments on acid denatured cyt c were carried out for transitions between U $\Rightarrow$ N and U $\Rightarrow$ MG states. Figure 4 shows the fluorescence (a) and ECD (b) detected time course of cyt c U $\Rightarrow$ N obtained by rapid neutralization with a 100 mM phosphate buffer solution at pH=6.8. Data were collected every 1 ms for 3 s after a dead time of 4 ms, and represent the average of signals from 10 and 30 shots for

fluorescence and CD, respectively. Stopped-flow fluorescence results (Figure 4a) fit a triple exponential curve, which is emphasized graphically by use of a log plot, consisting of a fast and two intermediate decays, with rate constants of k_1= 110, k_2= 7.2, and k_3=2.1 s^{-1}. However, stopped-flow ECD (Figure 4b) are best fit with a single exponential curve having an intermediate rate constant k= 6.3 s^{-1}. The fast fluorescence decay is not detectable in ECD, due to its longer dead time, and the slowest change is lost due to higher noise in ECD. In the refolding experiments performed at 15°C, we found that over 80% of the change in CD signal recorded at 222 nm was recovered and over 90% of the fluorescence signal was quenched within the 4 ms

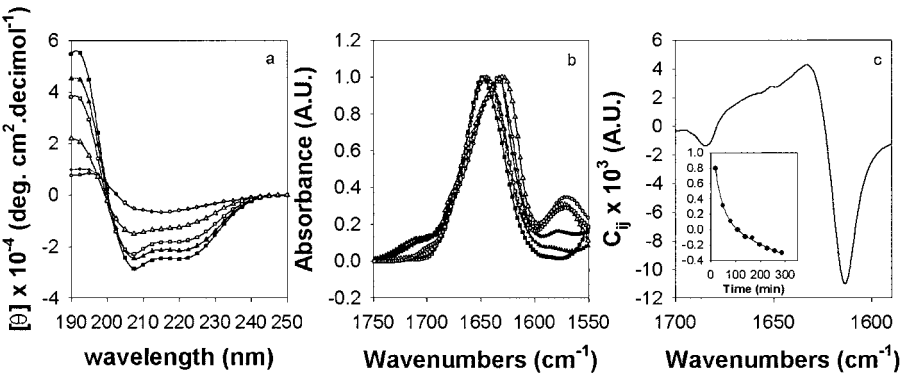

Figure 5. (a) ECD and (b) FTIR of β-lactglobulin under various conditions, pH=7 (open), pH=2 (filled) in H_2O (○), in 50% MeOH (Δ) and in 50% TFE (□). The time dependent IR in 50% MeOD is shown as the change (inset) in the second component (c, β-sheet).

mixing dead time, referred to as the "burst phase".[73] Nearly native levels of helical secondary structure and compact core (Tyr interaction) are formed on folding from the acid denatured state in less than 4 ms, which implies there is little barrier to helical formation. Since our equilibrium data show partially helical character in the acid denatured state, these results are consistent.

Alternate solvent experiments: Besides changing conformation due to pH or salt addition which can change the charge of the hetero polymer sequence, one can also create a partially ordered system by altering the solvent polarity or H-bonding capability. TFE and MeOH have long been used to reduce the solvent activity and affect the water H-bonding to the peptide backbone.

β-Lactoglobulin: Figure 5a and 5b show the far UV-ECD and amide I FTIR spectra of β-

lactoglobulin (β-LG) for neutral and low pH at room temperature with 50% (v/v) of Me-OD and TFE-OD, respectively. The ECD spectra (Figure 5a) show that β-LG has significant β-sheet structure (a negative peak at 215 nm and a positive peak at 194 nm)[74,75] at both pH 7 and 2 (circles), whose spectra completely overlap. When the protein is in 50% TFE or MeOH, the ECD gains α-helical characters (negative at 222 nm and 208 nm and a positive peak at ~192 nm). The β-LG in 50% TFE (square) has more ellipticity than in 50% methanol (triangle), suggesting TFE induces more partial α-helical ordering in this polypeptide sequence and more strongly shifts it from its native state.

FTIR spectra of β-LG show an amide I peak at 1633 cm^{-1} for both pH=7 and 2, being consistent with the ECD indication of a high β-sheet content. In 50% TFE, consistent with increased helix, the amide I shifts to ~1648 cm^{-1}. However, with 50% MeOD when pH=7, an amide I peak at ~1630 cm^{-1} is obtained, indicating more β-sheet character, disgreeing with the ECD. Curve fitting

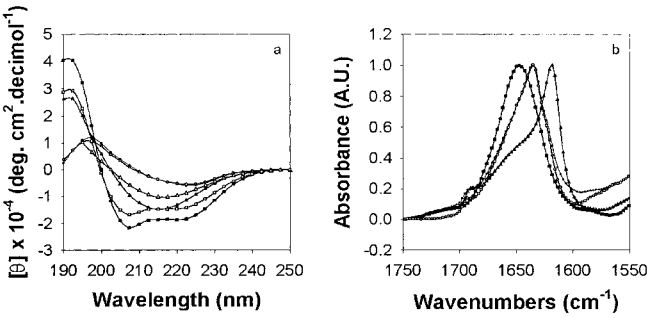

Figure 6. (a) ECD and (b) FTIR of concanavalin A under various conditions, pH=7 (open), pH=2 (filled) in H_2O (○), in 50% MeOH (Δ) and in 50% TFE (□).

and 2nd derivative analysis of this amide I band indicate a component at ~1650 cm^{-1}, suggesting partial α-helical conformation. More dilute β-LG (1mg/ml) has a peak ~1650 cm^{-1} (data not shown), indicating the ECD-IR difference is due to concentration. Factor analysis for the time dependent FTIR of β-LG in MeOD yields a β-sheet component (Figure 5c) whose contribution (loading), shown as an inset, is fit by a double exponential with k_1=0.037 and k_2=0.0033 min^{-1}. These optical spectral data confirm that the β-LG native state is not a sharply defined, highly ordered minimum energy structure since the native structure can be mutated to a highly α-helical one by solvent perturbation. None the less, this new structure is only partially ordered as seen by

the variable effect of alcohol and the ease of aggregation in the MeOH case. This latter situation implies that the hydrophobic parts of the polymer sequence are being exposed in alcohol by reducing the water activity. The native structure of β-LG is unusual, since simple prediction of helix or sheet propensity would suggest it should be helical.[76,77] Combining spectral methods and using bandshape analysis can detect the components shifting from β-sheet to α-helix forms.

Concanavalin A. Figure 6a and 6b show the ECD and FTIR spectra of concanavalin A (Con A) at pH=7 and 2 with 50% MeOH or TFE. In 50% TFE, the ECD spectra have characteristics of α-helical structure at both pH=7 and pH=2, differing sharply from the β-like ECD in water, which again suggests reordering of local structure, although Con A is a more stable sheet (having flatter, more extended strands) than β-LG. In contrast, Con A in 50% TFE at pH=7 began to precipitate after several hours, while in 50% MeOH, the Con A ECD retained β-sheet character. The amide I peak is observed for Con A at 1634 cm^{-1}, indicating an ordered (mostly β-sheet) structure. In 50% TFE, at pH=1.9, an amide I peak at 1648 cm^{-1} is observed, indicating conversion to partial α-helical order, consistent with the ECD. However, at pH=4.1 in 50% TFE, precipitation resulted, consistent with the ECD result, but with FTIR aggregation is accelerated by the higher concentration. Finally in 50% MeOH, at pH=1.9, a sharp peak at 1618 cm^{-1} as well as a shoulder peak at 1690 cm^{-1} are observed, which are usually assigned to intermolecular β-sheet structure and suggest local intramolecular to intermolecular β-sheet transition. Such an IR-

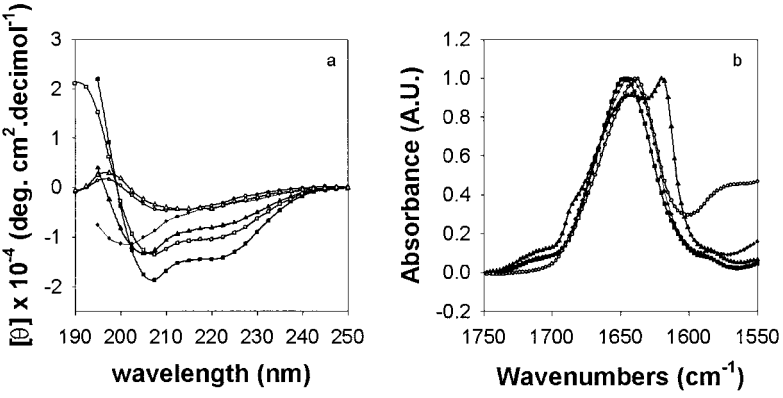

Figure 7. (a) ECD and (b) FTIR of carbonic anhydrase under various conditions, pH=7 (open), pH=2 (filled) in H_2O (○), in 50% MeOH (Δ) and in 50% TFE (□).

detectable change to an aggregate form is hard to differentiate with ECD.

Carbonic anhydrase. Figure 7a and 7b show the ECD and FTIR spectra of carbonic anhydrase (CA) at pH=7 and 2 with 50% MeOH or TFE. At pH=7, CA shows ECD typical of β-sheet structure, while at pH=2, a typical random coil spectrum is observed, suggesting complete acid denaturation of the β-sheet dominant structure, analogous to cyt c. In 50% TFE, spectra typical of α-helical structure are observed. The FTIR spectrum for CA at pH=6.1 shows an amide I peak at 1638 cm^{-1}, mostly β-sheet, and at pH=2 shifts to 1643.2 cm^{-1}, random coil, and in 50% TFE, the amide I is at 1647 cm^{-1}, α-helical, consistent with the ECD results. In 50% of MeOD, at pH=2, a sharp feature at 1619 cm^{-1} and a shoulder at ~1687 cm^{-1} indicate intermolecular β-sheet structure, while the broad band at ~1643 cm^{-1} remains, due to remaining random coil structure. The structure of CA can vary from native (presumably highly ordered) to partially helical, and from very little long range order (coil) to highly extended sheet (aggregate). These levels of partial order in the CA polymer are the structural response to charge repulsion, solvent polarity and H-bonding capability.

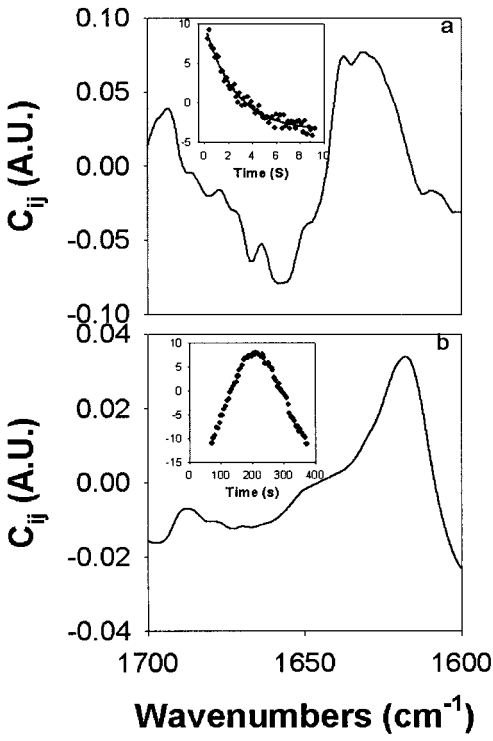

Figure 8. The second component spectrum of stopped-flow FTIR for concanavalin A (pH=4.1) mixing with TFE-OD (1:1) recorded for the fast change (a) and slow change (b). The corresponding coefficient loading changes with time are shown as insets.

Dynamic solvent mixing. Some of the long-range sensitive ECD results do not agree with the shorter range dependent FTIR data. For example, at neutral pH, concanvalin A in 50% TFE shows α-helical ECD, while with FTIR precipitation is observed which suggests β-structure. To further explore this, a stopped-flow FTIR experiment was

carried out, rapidly mixing Con A with TFE-OD in a 1:1 ratio at pH=4.1. A single FTIR spectrum is recorded every 80 ms for a total of ~10 s to detect the fast change, after that, a series of spectra with an average separation of 5 s are recorded to detect the slow change. Factor analysis results for the fast and slow change are shown in Figure 8. The fast change corresponds to disappearance of β-sheet and the growth of α-helix, with the ~1634 cm^{-1} feature decreasing and ~1656 cm^{-1} increasing with time. The corresponding change in coefficent loading (inset to Figure 8a) can be fit well with a single exponential curve, giving a rate constant of ~0.4 s^{-1}. The slow change (up to 200 s) shown in Figure 8b indicates the growth of absorbance at ~1617 cm^{-1} indicative of aggregation with k=1.7 min^{-1}. After that (200-400 s) a linear decrease is observed which is probably due to precipitation.

Conclusion

We have shown that various optical techniques, IR, VCD, ECD and fluorescence can be used to monitor the change in local order at different levels for protein based polypeptides. Due to their hetero-sequences, a wide variety of structures are possible within the same molecule, even in the native state, giving the concept of local order a new dimension. The electronic spectra based techniques (ECD, fluorescence) tend to sense longer range interactions while the vibrational ones (here IR, VCD) sense shorter range effects. This leads to a complementarity of information. Similarly, each technique has strengths and weaknesses in discriminating between various structural types. Thus, use of several of them in a combined study leads to more detailed interpretability. By perturbing the structure with solvent, pH, charge balance, temperature and other means, the stability of partially ordered states can be explained with a finer discrimination even though these techniques lack site-specific spatial resolution. Finally, the fast time scales inherent to optical spectra provide an opportunity to monitor dynamic changes in the structure in real time, allowing detailed kinetic analysis and the potential to develop mechanistic pictures for transitions between ordered, partially ordered and disordered states.

Acknowledgments

This research was supported in part by a grant from the Research Corporation.

1) G. D. Rose, Editor, "*Advances in Protein Chemistry*", 62, Academic Press, San Diego, 2002.
2) L. D. Barron, E. W. Blanch, L. Hecht, in: "*Advances in Protein Chemistry*", G. D. Rose, Ed., Academic, San Diego 2002, Vol. 62, p. 51-90.
3) A. T. Tu, "*Raman Spectroscopy in Biology*", Wiley, New York 1982.
4) L. D. Barron, L. Hecht, in: "*Circular dichroism, principles and applications*", K. Nakanishi, N. Berova, R. W. Woody, Ed., VCH Publishers, New York 1994, p. 179-215.
5) P. L. Polavarapu, "*Vibrational spectra: Principles and Applications with Emphasis on Optical Activity*", Elsevier, New York 1998, Vol. 85.
6) L. A. Nafie, T. B. Freedman, in: "*Circular Dichroism: Principles and Applications*" , 2nd ed., N. Berova, K. Nakanishi, R. W. Woody, Ed., Wiley, New York 2000, p. 97-131.
7) R. A. G. D. Silva, J. Kubelka, S. M. Decatur, P. Bour, T. A. Keiderling, *Proc. Natl. Acad. Sci. U. S. A.* **2000**, *97*, 8318-8323.
8) S. M. Decatur, J. Antonic, *J. Am. Chem. Soc.* **1999**, *121*, 11914-11915.
9) J. Kubelka, T. A. Keiderling, *J. Am. Chem. Soc.* **2001**, *123*, 6142-6150.
10) J. W. Brauner, C. Dugan, R. Mendelsohn, *J. Am. Chem. Soc.* **2000**, *122*, 677-683.
11) T. D. Anderson, J. Hellgeth, P. T. Lansbury Jr., *J. Am. Chem. Soc.* **1996**, *118*, 6540-6546.
12) R. Huang, J. Kubelka, W. Barber-Armstrong, R. A. G. D. Silva, S. M. Decatur, T. A. Keiderling, **submitted**.
13) W. C. Johnson, *Method. Enzymol.* **1992**, *210*, 426-447.
14) N. Sreerama, R. W. Woody, *J. Mol. Biol.* **1994**, *242*, 497-507.
15) N. J. Greenfield, *Anal. Biochem.* **1996**, *235*, 1-10.
16) S. Y. Venyaminov, J. T. Yang, in: "*Circular Dichroism and the Conformational Analysis of Biomolecules*" , G. D. Fasman, Ed., Plenum Press, New York 1996, p. 69-107.
17) R. W. Woody, in: "*Circular Dichroism and the Conformational Analysis of Biomolecules*" , G. D. Fasman, Ed., Plenum Press, New York 1996, p. 25-67.
18) W. C. Johnson, *Proteins* **1999**, *35*, 307-312.
19) M. Sreerama, S. Y. Venyaminov, R. W. Woody, *Anal. Bioch.* **2000**, *287*, 243-251.
20) Z. Shi, R. W. Woody, N. R. Kallenbach, in: "*Advances in Protein Chemistry*" , G. Rose, Ed., Academic, New York 2002, Vol. 62, p. 163-240.
21) J. R. Lakowicz, in: "*Modern Physical Methods in Biochemistry, Part B*" , A. Neuberger, L. L. M. Van Deenen, Ed., Elsevier, Amsterdam 1988, Vol. 11B.
22) P. I. Haris, D. Chapman, in: "*Infrared Spectroscopy of Biomolecules*" , H. H. Mantsch, D. Chapman, Ed., Wiley-Liss, Chichester 1996, p. 239-278.
23) F. S. Parker, "*Applications of Infrared, Raman and Resonance Raman Spectroscopy*", Plenum, New York 1983.
24) W. Surewicz, H. H. Mantsch, D. Chapman, *Biochemistry* **1993**, *32*, 389-394.
25) D. M. Byler, H. Susi, *Biopolymers* **1986**, *25*, 469-487.
26) M. Jackson, H. H. Mantsch, *Crit. Rev. Biochem. Mol. Biol.* **1995**, *30*, 95-120.
27) S. Krimm, J. Bandekar, *Adv. Protein Chem.* **1986**, *38*, 181-364.
28) S. Krimm, in: "*Biological Applications of Raman Spectroscopy, Vol 1: Raman Spectra and the Conformations of Biological Macromolecules*" , T. G. Spiro, Ed., Wiley, New York 1987, Vol. 1.
29) S. Krimm, in: "*Infrared Analysis of Peptides and Proteins: Principles and Applications. ACS Symposium Series*" , B. R. Singh, Ed., The American Chemical Society, Washington DC 2000, p. 38-53.
30) H. Torii, M. Tasumi, *J. Chem. Phys.* **1992**, *96*, 3379-3387.
31) P. Pancoska, L. Wang, T. A. Keiderling, *Protein Sci.* **1993**, *2*, 411-419.
32) M. Jackson, P. I. Haris, D. Chapman, *Biochemistry* **1991**, *30*, 9681-9686.
33) G. Martinez, G. Millhauser, *J. Struct. Biol.* **1995**, *114*, 23-27.
34) H. Fabian, C. Schultz, D. Naumann, O. Landt, U. Hahn, W. Saenger, *J. Mol. Biol.* **1993**, *232*, 967-981.
35) H. Fabian, C. Schultz, J. Backmann, U. Hahn, W. Saenger, H. H. Mantsch, D. Naumann, *Biochemistry* **1994**, *33*, 10725-10730.
36) D. M. Byler, D. L. Lee, C. S. Randall, in: "*Infrared Analysis of Peptides and Proteins: Principles and Applications. ACS Symposium Series*" , B. R. Singh, Ed., American Chemical Society, Washington DC 2000, p. 145-158.
37) F. Dousseau, M. Pezolet, *Biochemistry* **1990**, *29*, 8771-8779.
38) S. Krimm, W. C. Reisdorf Jr., *Faraday Disc.* **1994**, *99*, 181-194.
39) N. N. Kalnin, I. A. Baikalov, S. Y. Venyaminov, *Biopolymers* **1990**, *30*, 1273-1280.

40) J. Kubelka, R. A. G. D. Silva, P. Bour, S. M. Decatur, T. A. Keiderling, in: "*Chirality: Physical Chemistry. ACS Symposium Series*" , J. M. Hicks, Ed., Oxford University Press, New York 2002, p. 50-64.
41)H. Torii, M. Tasumi, in: "*Infrared Spectroscopy of Biomolecules*" , H. Henry, H. H. Mantsch, D. Chapman, Ed., Wiley-Liss, Inc 1996, p. 1-18.
42) D. C. Lee, P. I. Haris, D. Chapman, R. C. Mitchell, *Biochemistry* **1990**, *29*, 9185-9193.
43) R. W. Sarver, W. C. Kruger, *Anal. Biochem.* **1991**, *199*, 61-67.
44) R. Pribic, I. H. M. Van Stokkum, D. Chapman, P. I. Haris, M. Bloemendal, *Anal. Biochem.* **1993**, *214*, 366-378.
45) R. W. Williams, A. K. Dunker, *J. Mol. Biol.* **1981**, *152*, 783-813.
46) V. Baumruk, P. Pancoska, T. A. Keiderling, *J. Mol. Biol.* **1996**, *259*, 774-791.
47) R. A. Dluhy, S. M. Stephens, S. Widayati, A. D. Williams, *Spectrochim. Acta, Part A* **1995**, *51*, 1413-1447.
48) E. Goormaghtigh, J. M. Ruysschaert, in: "*Infrared Analysis of Peptides and Proteins: Principles and Applicantions. ACS Symposium Series*" , B. R. Singh, Ed., American Chemical Society, Washington DC 2000, p. 96-116.
49) P. J. Stephens, F. J. Devlin, C. S. Ashvar, C. F. Chabalowski, M. J. Frisch, *Faraday Discuss.* **1994**, *99*, 103-119.
50) T. A. Keiderling, in: "*Circular Dichroism: Principles and Applications*" , 2nd ed., N. Berova, K. Nakanishi, R. A. Woody, Ed., Wiley-VCH, New York 2000, p. 621-666.
51) L. A. Nafie, *Ann. Rev. Phys. Chem.* **1997**, *48*, 357-386.
52) P. Bour, J. Sopkova, L. Bednarova, P. Malon, T. A. Keiderling, *J. Comput.Chem.* **1997**, *18*, 646-659.
53) P. Bour, J. Kubelka, T. A. Keiderling, *Biopolymers* **2000**, *53*, 380-395.
54) J. Kubelka, R. A. G. D. Silva, T. A. Keiderling, *J. Am. Chem. Soc.* **2002**, *124*, 5325-5332.
55) J. Hilario, J. Kubelka, T. A. Keiderling, *J. Am . Chem. Soc.* **2003**, *125*, 7562-7574.
56) T. A. Keiderling, in: "*Circular Dichroism and the Conformational Analysis of Biomolecules*" , G. D. Fasman, Ed., Plenum, New York 1996, p. 555-598.
57) P. Pancoska, E. Bitto, V. Janota, M. Urbanova, V. P. Gupta, T. A. Keiderling, *Protein Sci.* **1995**, *4*, 1384-1401.
58) L. Wang, Ph.D. thesis, University of Illinois at Chicago, Chicago, 1993.
59) T. A. Keiderling, J. Kubelka, J. Hilario, in: "*Vibrational spectroscopyy of polymers and biological systems*" , M. Braiman, V. Gregoriou, Ed., Marcel Dekker Publ., Amsterdam-New York 2003, Vol. in press.
60) T. A. Keiderling, in: "*Practical Fourier Transform Infrared Spectroscopy*" , K. Krishnan, J. R. Ferraro, Ed., Academic Press, San Diego 1990, p. 203-284.
61) A. Ikai, W. Fish, C. Tanford, *J. Mol. Biol.* **1973**, *73*, 165-184.
62) A. L. Fink, L. J. Calciao, Y. Goto, T. Kurotsu, D. Palleros, *Biochemistry* **1994**, *33*, 12504-12511.
63) E. Stellwagen, J. Babul, *Biochemistry* **1975**, *14*, 5135-5140.
64) Y. Goto, L. Calciano, A. L. Fink, *Proc. Natl. Acad. Sci. U.S.A.* **1990**, *87*, 573-577.
65) M. F. Jeng, S. W. Englander, G. A. Elove, A. J. Wand, H. Roder, *Biochemistry* **1990**, *29*, 10433-10437.
66) A. A. Ismail, H. H. Mantsch, P. T. Wong, *Biochim. Biophys. Acta* **1992**, *1121*, 183-188.
67) A. H. Clark, D. H. P. Saunderson, A. Sugget, *Int. J. Peptide Res.* **1981**, *17*, 353-364.
68) T. Y. Tsong, *Biochemistry* **1973**, *12*, 2209-2214.
69) R. K. Dukor, T. A. Keiderling, *Biopolymers* **1991**, *31*, 1747-1761.
70) T. A. Keiderling, Q. Xu, in: "*Adnances in protein chemistry: unfolded proteins*" , G. D. Rose, Ed., Academic Press, San Diego 2002, Vol. 62, p. 111-161.
71) Y. Goto, N. Takahashi, A. L. Fink, *Biochemistry* **1990**, *29*, 3480-3488.
72) Y. Goto, Y. Hagihara, D. Hamada, M. Hoshino, I. Nishii, *Biochemistry* **1993**, *32*, 11878-11885.
73) K. Kuwajima, E. P. Garvey, B. E. Finn, C. R. Matthews, S. Sugai, *Biochemistry* **1991**, *30*, 7693-7703.
74) M. Z. Papiz, L. Sawyer, E. E. Eliopoulos, A. C. T. North, J. B. C. Findlay, R. Sivaprasadarao, T. A. Jones, M. E. Newcomer, P. J. Kraulis, *Nature (London)* **1986**, *324*, 383-395.
75) H. L. Monaco, G. Zanotti, P. Spadon, M. Bolognesi, L. Sawyer, E. E. Eliopoulos, *J. Mol. Biol.* **1987**, *197*, 695-706.
76) K. Shiraki, K. Nishikawa, Y. Goto, *J. Mol. Biol.* **1995**, *245*, 180-194.
77) K. Nishikawa, T. Noguchi, *Methods Enzymol.* **1991**, *202*, 31-44.